

Time Course of Benoxacor Metabolism and Identification of Benoxacor Metabolites Isolated from Suspension-Cultured *Zea mays* Cells 1 h after Treatment[†]

Keith D. Miller,^{*,‡,§} Gerard P. Irzyk,^{‡,||} E. Patrick Fuerst,[‡] Janis E. McFarland,[‡]
Michael Barringer,[‡] Shawn Cruz,[‡] William J. Eberle,[‡] and Werner Föry[#]

Department of Crop and Soil Sciences, Washington State University, Pullman, Washington 99164-6420, Environmental Metabolism, Agricultural Division, Ciba Crop Protection, Greensboro, North Carolina 27419-8300, and Ciba Crop Protection, Ciba-Geigy Ltd., CH-4002 Basle, Switzerland

Extracts of suspension-cultured *Zea mays* (cv. Black Mexican Sweet) cells treated with [¹⁴C]benoxacor for 0.25–24 h were analyzed by HPLC and TLC to investigate the metabolic fate of benoxacor. Thin layer chromatography determined that benoxacor was rapidly metabolized to six detectable metabolites within 0.5 h. Twelve metabolites were detected in extracts from cells treated for 24 h. Analysis of cell extracts by reversed phase HPLC determined that the glutathione conjugate [mono(GSH)] of benoxacor was present in all samples analyzed, based on cochromatography with a mono(GSH) conjugate standard. The abundance of the mono(GSH) conjugate increased as treatment time increased. The presence of a di(GSH) conjugate was detected in extracts of cells treated for 0.5 h and reached a maximum level 2 h after treatment. Three predominant metabolites present in samples treated with benoxacor for 1 h were subjected to structural analysis by ¹H-NMR or mass spectrometry following purification by conventional HPLC methodologies. These structural analyses determined that two of the metabolites were the catabolic formylcarboxamide and carboxycarboxamide derivatives of benoxacor. A third metabolite was determined to be the mono(GSH) conjugate of benoxacor. This metabolite consisted of a single glutathione molecule linked via the cysteinyl sulfhydryl group to the *N*-dichloroacetyl α -carbon of benoxacor. Structures of the metabolites and postulated pathways of their biosynthesis *in vivo* are presented.

Keywords: *Benoxacor; herbicide safener; CGA-154281; glutathione S-transferase; BMS cells; xenobiotic metabolism; xenobiotic detoxification; maize; dehalogenase/dechlorinase enzymes; glutathione conjugation; dichloroacetamide; substituted benzoxazine; herbicide safener metabolism*

INTRODUCTION

Benoxacor [4-(dichloroacetyl)-3,4-dihydro-3-methyl-2*H*-1,4-benzoxazine] is a dichloroacetamide safener that protects maize seedlings against the potential of early injurious effects from the herbicide metolachlor [2-chloro-*N*-(2-ethyl-6-methylphenyl)-*N*-(2-methoxy-1-methylethyl)-acetamide]. Benoxacor functions by increasing the activity of glutathione *S*-transferase (GST, EC 2.5.1.18) isozymes, which subsequently conjugate metolachlor to the endogenous tripeptide glutathione (γ -L-glutamyl-L-cysteinylglycine), yielding a less phytotoxic or nonphytotoxic glutathione–metolachlor conjugate (Viger *et al.*, 1991; Dean *et al.*, 1991; Irzyk and Fuerst, 1993; Fuerst *et al.*, 1993; Miller *et al.*, 1994).

The biochemical events leading to safener (benoxacor or others)-mediated increases of GST activity are un-

known. It has been suggested that commercial safeners are actually “prosafeners” which must initially be metabolized to an active form to elicit a specific biochemical response (Kömives and Hatzios, 1991; Dutka, 1991). Unfortunately, data on safener metabolism, or the effects of safener metabolites on eliciting increases of GST activity, are limited. Miaullis *et al.* (1978) documented the metabolism of the dichloroacetamide safener dichlormid (*N,N*-diallyl-2,2-dichloroacetamide) to alcohol, aldehyde, and carboxylic acid derivatives in 8-day-old maize plants 48 HAT. Similarly, Breaux *et al.* (1989) documented the metabolism of the thiazole safener flurazole [phenylmethyl 2-chloro-4-(trifluoromethyl)-5-thiazolecarboxylate] to alcohol and carboxylic acid derivatives, as well as a GSH conjugate, in 3–5 day-old maize and sorghum plants treated for 2 h. Since dichlormid and flurazole are metabolized in maize seedlings, and because they both increase GST activity in maize, we wished to determine if benoxacor was metabolized in maize cell suspension cultures.

As a precursory step to determine the mechanism by which benoxacor increases GST activity in maize, the metabolic fate of [¹⁴C]benoxacor was studied in a model system of maize cell suspension cultures. Specifically, the objectives of the present study were to (1) study the *in vivo* metabolism of [¹⁴C]benoxacor from 0.25 to 24 HAT using TLC and HPLC, (2) use conventional HPLC methodologies to isolate and purify three [¹⁴C]benoxacor metabolites present 1 HAT, (3) determine the chemical structure of the purified metabolites using ¹H-NMR or mass spectrometry, and (4) propose pathways by which

* Author to whom correspondence should be addressed (e-mail kdmiller@wsu.edu).

[†] Contribution from the Department of Crop and Soil Sciences, Washington State University, College of Agriculture and Home Economics; Departmental Paper 9604-07.

[‡] Washington State University.

[§] Present address: Plant Biochemistry Research and Training Center, Washington State University, Pullman, WA 99164-6340.

^{||} Present address: Mycogen Corp., 5501 Oberlin Dr., San Diego, CA 92121.

[‡] Ciba Crop Protection, Greensboro.

[#] Ciba Crop Protection, Basle.

the identified metabolites formed *in vivo*. The advantages of using cell-suspension cultures versus intact plants for xenobiotic metabolite isolation have been previously discussed (Miller *et al.*, 1994). The identification of the most abundant benoxacor metabolites extracted from maize cells 3 and 24 HAT is presented elsewhere (Miller *et al.*, 1996).

MATERIALS AND METHODS

Chemicals. Analytical grade unlabeled (>98% purity) and phenyl-¹⁴C-labeled (99% purity) benoxacor (11.34 or 2.24 μ Ci μ mol⁻¹) and [4-(chloroacetyl)-3,4-dihydro-3-methyl-2H-1,4-benzoxazine] (CGA-146468) were synthesized by Ciba Corp. Reduced [*glycine*-2-³H]glutathione (43.8 μ Ci μ mol⁻¹) was obtained from DuPont NEN, Inc. HPLC and reagent grade solvents were acquired from Fisher Scientific. Liquid scintillation reagents were obtained from Amersham Corp. (BCS scintillation cocktail), Fisher Scientific (Scintiverse BD), or Beckman Instruments (Ready-Flow). All other chemicals were obtained from Sigma Chemical Co. (St. Louis, MO).

Cell Culture Maintenance and Treatment with [¹⁴C]-Benoxacor. Maize cells (cv. Black Mexican Sweet) were maintained in Murashige and Skoog liquid media as previously described (Miller *et al.*, 1994). Middle log-phase cell cultures for both the TLC and HPLC experiments examining the metabolic fate of benoxacor over time were aseptically treated with 10 μ M [¹⁴C]benoxacor and harvested 0.5, 1, 2, 3, 12, and 24 HAT (TLC experiment) or 0.25, 0.5, 1, 2, 3, and 6 HAT (HPLC experiment), as previously described (Miller *et al.*, 1994). Treated cells were harvested by vacuum filtration, rinsed with water, frozen in liquid nitrogen, and stored at -80 °C until extraction.

For large-scale metabolite isolations, 5 L of 7-day-old (middle log-phase) cell cultures were treated with 11.5–13 nCi mL⁻¹ of 100 μ M [¹⁴C]benoxacor (0.114–0.167 μ Ci μ mol⁻¹) and allowed to incubate on a gyratory shaker for 1 h. Treated cells were harvested by vacuum filtration, rinsed once with water, and stored at -196 °C until extraction. Amounts of 80–100 g of cells were routinely obtained from 5 L of 7-day-old cell cultures.

Time Course of [¹⁴C]Benoxacor Metabolism. Harvested cells were extracted with 5 volumes of 80% (v/v) acetonitrile in a glass mortar and pestle to yield the crude homogenate. The crude homogenate was centrifuged at 12000g for 5 min to pellet cell debris, and radioactivity in an aliquot of the decanted supernatant was quantified by LSC. Aliquots containing 10 000 cpm of each extract were spotted onto the preabsorbent zone of a precoated analytical TLC plate (Whatman F-254 silica, channeled, 250 μ m coating thickness), and benoxacor metabolites were resolved from benoxacor using either (I) chloroform/methanol/formic acid/water (75:25:4:2 v/v/v) or (II) 1-butanol/acetic acid/water (60:15:25 v/v/v). To detect radioactive metabolites, the plate was placed in contact with autoradiographic film (Hyperfilm, Amersham, Inc.) for 25 days at room temperature or scanned for 16–20 h using a radioanalytic image scanner (Ambis).

To monitor benoxacor metabolism over time using reversed phase HPLC, cells were extracted with 80% (v/v) acetonitrile and centrifuged as previously described. Acetonitrile in the crude homogenate was evaporated under nitrogen at ambient temperature. After radioactivity in an aliquot of the extract was quantified by LSC, volumes containing 50 000 cpm were adjusted to 0.0125% (v/v) TFA and injected onto an analytical C₁₈ HPLC column (Alltech Econosphere, 5 μ m, 4.6 \times 250 mm), previously equilibrated in 0.0125% (v/v) TFA, at a flow rate of 1.0 mL min⁻¹ (see Preparative HPLC for instrumentation). The following gradient was then used to resolve benoxacor metabolites from unmetabolized benoxacor: [solvent A = 0.0125% (v/v) TFA; solvent B = MeOH/0.0125% (v/v) TFA] 0–3 min, 0% B; 3–5 min, 0–20% B; 5–25 min, 20% B; 25–85 min, 20–100% B. Radioactivity eluted from the column was monitored using a Beckman 171 radioisotope detector equipped with a 1000 μ L flow cell suitable for liquid samples. Scintillation cocktail (Beckman Ready-Flow) was mixed with the

Table 1. HPLC Gradients Used for the Purification of Benoxacor Metabolites Isolated from Maize Cells 1 HAT

gradient	conditions ^a
1	0–3 min, 0% B; 3–23 min, 0–100% B; 23–30 min, 100% B
2	0–3 min, 0% B; 3–8 min, 0–50% B; 8–30 min, 50% B isocratic grad
3	0–3 min, 0% B; 3–7 min, 0–40% B; 7–30 min, 40% B isocratic grad
4	0–3 min, 0% B; 3–6 min, 0–30% B; 6–30 min, 30% B isocratic grad
5	0–5 min, 0% B; 5–35 min, 0–100% B; 35–60 min, 100% B, no TFA in mobile phase

^a Solvent A = 0.01% (v/v) TFA; solvent B = acetonitrile/0.01% (v/v) TFA.

HPLC eluent at a flow rate of 2.0 mL min⁻¹ prior to entering the flow cell.

Large-Scale Metabolite Extraction and Preparation. The crude homogenate and component metabolite fractions were maintained at 0 °C except for partitioning, SPE, and HPLC procedures or unless otherwise stated. Frozen cells were homogenized in 5 volumes of 80% (v/v) acetonitrile using a Waring blender at the highest speed (5 \times 60 s pulses) to yield the crude homogenate. The crude homogenate was centrifuged at 3000g for 15 min to pellet cell debris, and the volume of the decanted supernatant was reduced *in vacuo* at 30 °C using a rotary evaporator. The resulting extract was then partitioned against 1 volume of chloroform and centrifuged to separate the two phases. The volume of the aqueous phase was further reduced *in vacuo* at 30 °C as previously described and manually loaded onto a preparative C₁₈ cartridge (SepPak, Waters Inc.) previously equilibrated with water. The column (~1 mL bed volume) was washed with 3 volumes of water, and radioactivity was eluted stepwise with 5 volumes each of 30, 50, 80, and 100% (v/v) acetonitrile. The majority (*i.e.* >90%) of radioactivity eluted from the cartridge prior to the 50% acetonitrile eluent. The 30–100% acetonitrile cartridge eluents containing radioactivity were pooled, their volume was reduced as previously described, and they were stored at -20 °C until HPLC analysis.

The volume of the chloroform phase was reduced to about 0.5 mL by rotary evaporation as previously described, diluted with 3 mL of acetonitrile, and briefly evacuated to remove the chloroform. The sample was then diluted with 10 volumes of water and loaded onto a preparative C₁₈ cartridge (SepPak, Waters, Inc.) previously equilibrated with water. Radioactivity was eluted stepwise with 5 volumes each of 50, 70, 90, and 100% (v/v) acetonitrile. The majority (*i.e.* >95%) of radioactivity eluted from the cartridge prior to the 90% acetonitrile eluent. The cartridge eluents containing radioactivity were pooled, their volumes reduced as previously described, and then stored at -20 °C until HPLC analysis.

Preparative HPLC. The HPLC system used in this study consisted of two Beckman Model 110B pumps, a 406 analog interface module (for computerized gradient programming), and a Beckman Model 165 variable wavelength detector set to monitor absorbance at 254 nm. Samples were adjusted to 0.01% (v/v) TFA and loaded onto a 0.01% (v/v) TFA-equilibrated Alltech Econosphere C₁₈ reversed phase preparative HPLC column (10 \times 250 mm) at a flow rate of 3 mL min⁻¹. Column eluent was collected in 3 mL fractions, and radioactivity in an aliquot of each fraction was quantified by LSC.

Gradients 1–4 (Table 1) were used sequentially to partially purify aqueous-soluble ¹⁴C-labeled metabolites. Samples were chromatographed using gradient 4 two to three times prior to analytical HPLC. Chloroform-soluble radioactivity was partially purified using gradients 1 and 2 (Table 1). Samples were chromatographed using gradient 2 two to three times prior to analytical HPLC.

Analytical HPLC. The previously described HPLC instrumentation used for preparative HPLC was also used for analytical HPLC except that samples were chromatographed through an Alltech Econosphere C₁₈ reversed phase analytical

HPLC column (4.6 × 250 mm) at a flow rate of 1.0 mL min⁻¹. Reversed phase analytical HPLC of samples partially purified by preparative HPLC was accomplished using, in sequence, gradients 1, 3, and 4 (Table 1). Samples were rechromatographed using gradients 3 and 4 two to three times prior to structural analyses.

HPLC/Mass Spectrometry. LC-ESI/MS and MS/MS spectra were obtained using a Perkin-Elmer Sciex API III triple-quadrupole mass spectrometer operated in the positive-ion mode. The electrospray assembly was operated between 4500 and 5500 V with an orifice potential of 60–80 V. Open-collision-cell type MS/MS experiments were conducted using argon as the collision gas at an ionization energy of 40–60 eV. Samples were chromatographed on a Spherisorb ODS(2) analytical HPLC column (Phase Separations, 2 × 150 mm) using a mobile phase of 20% (v/v) MeOH at a flow rate of 0.4 mL min⁻¹ prior to entering the source.

LC-EI/MS spectra of selected samples were generated using a Hewlett-Packard 1090 liquid chromatographic system coupled to a HP 5989A mass spectrometer by a 59980B particle beam interface. Ionization was achieved by electron impact at 70 eV. Samples were chromatographed on an Alltech Econosphere C₁₈ reversed phase analytical HPLC column (4.6 × 250 mm) at a flow rate of 0.5 mL min⁻¹ using a mobile phase of 40% (v/v) acetonitrile/0.01% (v/v) TFA prior to entering the source.

Gas Chromatography–Mass Spectrometry. GC-EI/MS spectra of selected samples were obtained using a HP 5890 Series II GC coupled to a HP5989A mass spectrometer. Ionization was achieved by electron impact at 70 eV. Prior to entering the source, samples were separated on a DB-5 microbore capillary column (J&W Scientific) using the following stepped thermal gradient: 0–3 min, 50 °C; 3–23 min, 50–250 °C; 23–25.8 min, 250–320 °C; 25.8–29 min, 320 °C.

Nuclear Magnetic Resonance Spectroscopy. One-dimensional ¹H-NMR and two-dimensional ¹H-NMR COSY experiments were conducted using a Bruker AMX-400 NMR spectrometer operating at a frequency of 400.13 MHz and temperatures of 289, 323, or 335 K. Samples were completely dried under nitrogen and subsequently dissolved in ACN-d₃ or D₂O prior to analysis.

Synthesis of Selected Analytical Standards. The mono-(GSH) conjugate of benoxacor was synthesized *in vitro* in 3 mL of distilled water containing 600 μmol of TAPS buffer (unadjusted pH of ~10.5) and 30 μmol of reduced [³H]-glutathione (0.33 μCi μmol⁻¹). The reaction was initiated by adding 1.5 μmol of 4-(chloroacetyl)-3,4-dihydro-3-methyl-2*H*-1,4-benzoxazine (dissolved in dimethyl sulfoxide) and then incubated at 30 °C for 16 h. The end-point of the reaction was not monitored over time, but the yield of the mono(GSH) conjugate in the crude reaction mixture was >95% as determined by analytical HPLC. The reaction was terminated by adding 30 μL of glacial acetic acid, and the reaction mixture was then partitioned against 0.5 volume of chloroform. The most abundant reaction product in the resulting aqueous phase was purified by HPLC using gradient 5 (Table 1). ¹H-NMR and COSY spectra as well as LC-ESI/MS spectral data confirmed this reaction product as the mono(GSH) conjugate of benoxacor.

The formylcarboxamide derivative [4-(formylcarbonyl)-3,4-dihydro-3-methyl-2*H*-1,4-benzoxazine] of benoxacor was synthesized in a total volume of 5 mL of distilled water containing 1 mmol of TAPS buffer (unadjusted pH of ~10.5) and 25 μmol of reduced glutathione. The reaction was initiated by adding 0.5 μmol of [¹⁴C]benoxacor (5.67 μCi μmol⁻¹). The reaction was incubated for 16 h at 30 °C and was then terminated by adding 50 μL of glacial acetic acid. The reaction mixture was partitioned against 0.5 volume of chloroform to remove unreacted benoxacor. The most abundant reaction product in the resulting aqueous phase was purified by HPLC using gradient 5 (Table 1). LC-EI/MS and GC-EI/MS spectra confirmed this compound as the formylcarboxamide derivative of benoxacor.

RESULTS AND DISCUSSION

Time Course of [¹⁴C]Benoxacor Metabolism.

Figure 1 illustrates HPLC analyses of crude extracts from [¹⁴C]benoxacor-treated BMS cells. Unmetabolized benoxacor was the most abundant radioactive compound 0.25, 0.5, and 1 HAT. Fifteen minutes after benoxacor treatment, one well-resolved metabolite accounted for 11% of the total extracted radioactivity and 34% of ¹⁴C-labeled metabolites (Figure 1A). This metabolite cochromatographed with the synthetic mono(GSH) conjugate. Also present in the chromatogram were two peak clusters which were presumably composed of several unresolved metabolites. By 30 min after treatment, the mono(GSH) conjugate accounted for about 27% of the total extracted radioactivity and 53% of ¹⁴C-labeled metabolites (Figure 1B). One additional metabolite present 30 min after treatment (retention time = 17 min) accounted for about 14% of the total extracted radioactivity and 26% of ¹⁴C-labeled metabolites and was later determined to be the di(GSH) conjugate of benoxacor (Miller *et al.*, 1996). By 2 HAT, the abundance of the di(GSH) conjugate reached its maximum level, accounting for 30% of the total extracted radioactivity and 38% of ¹⁴C-labeled metabolites (Figure 1D). By 3 and 6 HAT, the di(GSH) conjugate comprised about 28% and 20%, respectively, of the total extracted radioactivity and 35% and 23%, respectively, of ¹⁴C-labeled metabolites (Figure 1E,F). By 3 and 6 HAT, the mono(GSH) conjugate accounted for about 35% and 46%, respectively, of the total extracted radioactivity, whereas it accounted for 43% and 53%, respectively, of ¹⁴C-labeled metabolites (Figure 1E,F). Due to the presence of a shoulder on the mono(GSH) conjugate peak in the 3 and 6 HAT samples, it is probable that at least one different metabolite cochromatographed with the mono(GSH) conjugate. Therefore, the integration data used for peak quantitation may overestimate the amount of mono(GSH) conjugate that is present in these samples.

TLC was also used since it allowed a qualitative comparison of chromatographically resolved metabolites in multiple samples. TLC of extracts from cells treated for 0.5–24 h with [¹⁴C]benoxacor are presented in Figure 2. TLC of extracts from cultures treated with benoxacor for 0.5 h resolved six detectable metabolites, while the number increased to 12 metabolites by 24 HAT. The presence of transient metabolites at some time points (*e.g.* Figure 2A: samples 0.5–3 HAT, third arrow from top; samples 12 and 24 HAT, sixth and eighth arrows from top) suggested that some of the benoxacor metabolites formed either are unstable or are intermediates that are consumed as substrates of other enzymes in the pathway of benoxacor metabolism.

Structural Analyses and Identification of Metabolites. *Benoxacor.* For reference, the LC-EI/MS spectrum of the benoxacor reference standard along with its deduced fragmentation pattern is depicted in Figure 3. The molecular ion was present at *m/z* 259/261/263 in the expected isotopic abundance ratio of 9:6:1 for a molecule with two chlorine atoms. High-mass fragment ions were observed at *m/z* 224/226, 176, 148, 134, and 120. The fragment ion at *m/z* 134 is due to the loss of both the dichloroacetyl group and the benzoxazine ring 3-position methyl group from the molecular ion. The base peak in this spectrum present at *m/z* 120 was used, in addition to the *m/z* 134 fragment ion, to search for benoxacor-related compounds in the

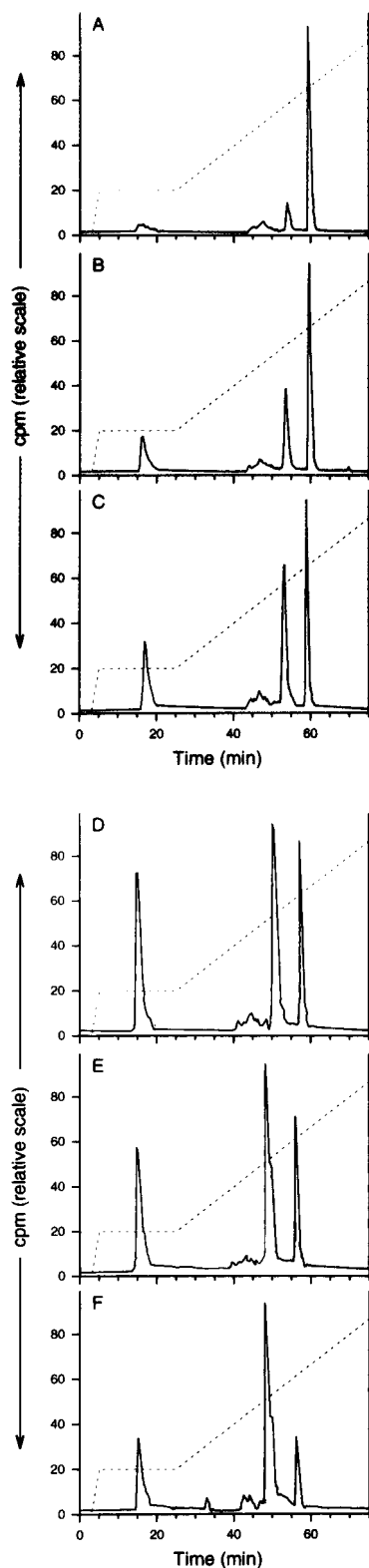


Figure 1. Time course of [^{14}C]benoxacor metabolism analyzed by reversed phase HPLC. Maize cells were treated with $10\ \mu\text{M}$ [^{14}C]benoxacor and harvested at the indicated times after treatment. Harvested cells were homogenized in 80% (v/v) acetonitrile, and radioactivity in an aliquot of the resulting extract was quantified by LSC. Aliquots containing 50 000 cpm of the extract were adjusted to 0.0125% (v/v) TFA and subjected to the gradient previously described. The elution of radioactivity was monitored using a radioisotope detector. Each chromatogram represents an extract from cells treated for (A) 0.25, (B) 0.5, (C) 1, (D) 2, (E) 3, and (F) 6 h with [^{14}C]benoxacor. Retention times: benoxacor, 59 min (57 min, D–F); mono(GSH) conjugate, 54 min (50 min, D–F); formylcarboxamide metabolite, 48 min (44 min, D–F); di(GSH) conjugate, 17 min (15 min, D–F).

total ion chromatograms and spectra of metabolite samples analyzed by LC-EI/MS.

One-dimensional $^1\text{H-NMR}$ spectra of the benoxacor reference standard yielded resonances with chemical shift values from δ 1 to 8. The carbon atom numbering scheme of the benoxacor molecule is provided in Figure 3. Specific assignments are as follows: δ 1.22 (C9, d, 3H), 4.24 (C2, d, 2H), 4.69 (C3, b, 1H), 6.78 (C11, s, 1H), 6.9–7.0 (C7 and C8, c, 2H), 7.17 (C6, t, 1H), and 7.61 (C5, b, 1H).

Unmetabolized [^{14}C]benoxacor was isolated and purified from the chloroform phase of the partition step in the purification procedure and accounted for about 33% of the total quantity of radioactivity 1 HAT. The $^1\text{H-NMR}$ and mass spectra of the extracted compound were identical to that of the benoxacor reference standard.

Formylcarboxamide Metabolite [4-(Formylcarbonyl)-3,4-dihydro-3-methyl-2H-1,4-benzoxazine]. The mass spectrum of this compound was obtained by GC-EI/MS and is illustrated in Figure 4. The molecular ion was present at m/z 205, with high-mass fragment ions at m/z 176, 148, 134, and 120. The fragment ion at m/z 176 corresponds to the loss of a formyl group from the molecular ion. The remaining fragmentation pattern is the same as the previously described benoxacor standard.

There are at least two hypothetical pathways through which the formylcarboxamide metabolite could form *in vivo*. In the first pathway, reductive dehalogenation of the dichloroacetyl α -carbon atom would precede an oxygenation reaction to form the formylcarboxamide metabolite. The oxygenation reaction could be catalyzed by a cytochrome P_{450} monooxygenase enzyme. Cytochrome P_{450} monooxygenase isozymes present in plants are known to hydroxylate both naturally occurring (Butt and Lamb, 1981; Donaldson and Luster, 1991) and xenobiotic molecules (Jones and Caseley, 1989; Donaldson and Luster, 1991). A hydroxylation reaction would subsequently require oxidation either by a separate oxidase enzyme or by a monooxygenase enzyme in a mixed oxidase–monooxygenase reaction.

The second proposed pathway describes how GST enzymes might catalyze formation of the formylcarboxamide metabolite via a dechlorination mechanism and is illustrated in a portion of Figure 5. The first step of this pathway consists of a GSH-dependent, GST-catalyzed reaction eliminating one chlorine atom from benoxacor to yield a resonance-stabilized chlorinated carbanion intermediate, represented as the corresponding enolate, and an electrophilic *S*-(chloro)GSH conjugate (Figure 5-II). Nucleophilic attack of the chlorinated glutathionyl sulfur atom (Figure 5-IIa) by the carbanion intermediate would then yield an α -chloro-*S*-(benoxacor)glutathione conjugate (Figure 5-IIIa). Enzyme-catalyzed or spontaneous hydrolysis of this reactive α -halothioether derivative would subsequently yield a putatively unstable *gem*-diol (Figure 5-IVa), which after dehydration would form the formylcarboxamide metabolite (Figure 5-V).

Prapanthadara *et al.* (1993) reported that several semipurified GST-C activities extracted from the mosquito *Anopheles gambiae* also had dehydrochlorinase activity when assayed with the insecticide substrate 1,1,1-trichloro-2,2-bis(*p*-chlorophenyl)ethane (DDT). They concluded that in all cases the DDT-dehydrochlorinase activities copurified with a GST-C activity and that GST isozymes were indeed responsible for the partial dechlorination of DDT. Similarly, Clark and Shamaan (1984)

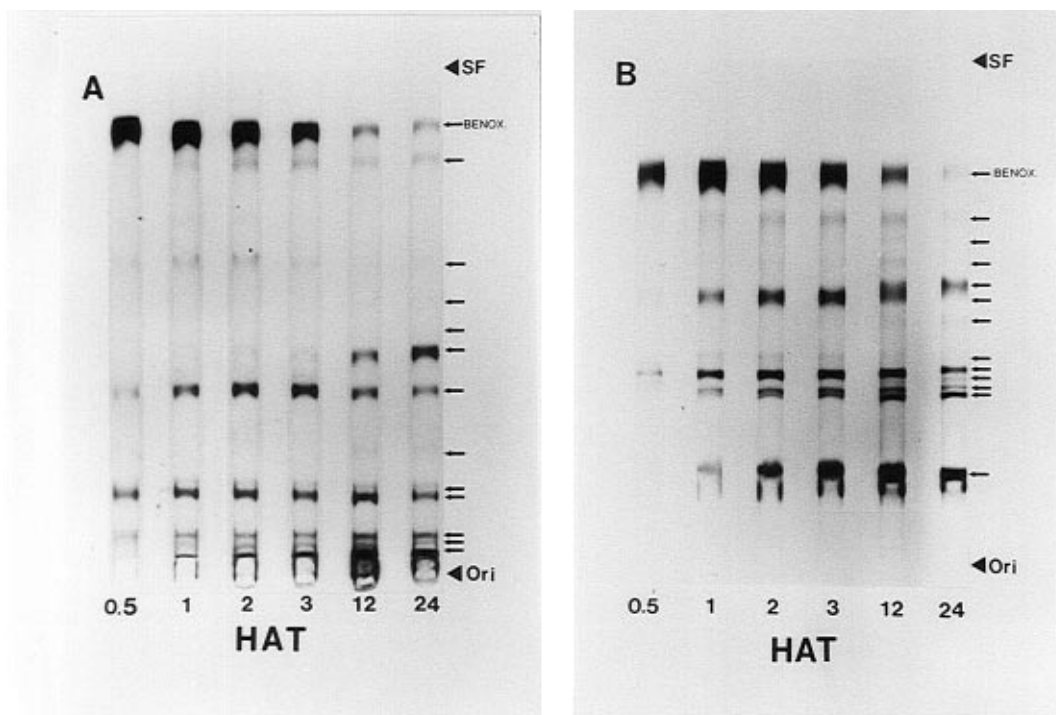


Figure 2. Time course of [^{14}C]benoxacor metabolism analyzed by TLC. Maize cells were treated with $10\ \mu\text{M}$ [^{14}C]benoxacor and harvested at the indicated times after treatment. Harvested cells were homogenized in 80% (v/v) acetonitrile, and radioactivity in an aliquot of the resulting extract was quantified by LSC. Aliquots containing 10 000 cpm of the extract were spotted onto a TLC plate and developed using (A) solvent system I or (B) solvent system II as previously described. Developed plates were placed into contact with X-ray film for 25 days to visualize radioactive metabolites. Ori, origin; SF, solvent front; BENOX, benoxacor (determined by cochromatography with the analytical standard). Arrows point to a metabolite present in one or more of the six samples.

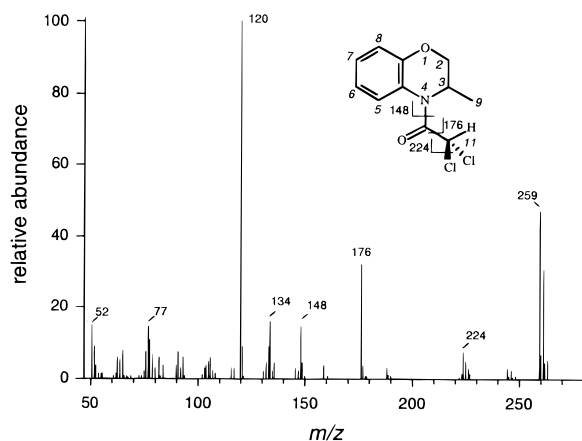


Figure 3. LC-EI/MS spectrum and partial fragmentation pattern of the benoxacor reference standard. The standard was subjected to HPLC using a 40% ACN/0.01% TFA isocratic gradient prior to entering the source. The carbon atom numbering scheme (italicized numbers) of the benoxacor molecule is provided on the structure to cross-reference $^1\text{H-NMR}$ spectra chemical shift assignments provided in the text.

determined that specific GSTs from the housefly *Musca domestica* also had dehydrochlorinase activity when assayed with the substrate DDT. Martin *et al.* (1980) proposed that chloramphenicol [(1*R*,2*R*)-(+)-1-(*p*-nitrophenyl)-2-(dichloroacetamido)-1,3-propanediol] and thiamphenicol [(1*R*,2*R*)-1-(*p*-methylsulfonyl)-2-(dichloroacetamido)-1,3-propanediol] were dechlorinated by a rat liver cytosol enzyme to a chloramphenicol-aldehyde derivative in a GSH-dependent reaction. Miaullis *et al.* (1978) used a GSH-free total soluble protein fraction from rat liver and determined that dichlorimid was metabolized *in vitro* to *N,N*-diallylgyoxylamide if GSH was added to the reaction mixture. If GSH, the protein

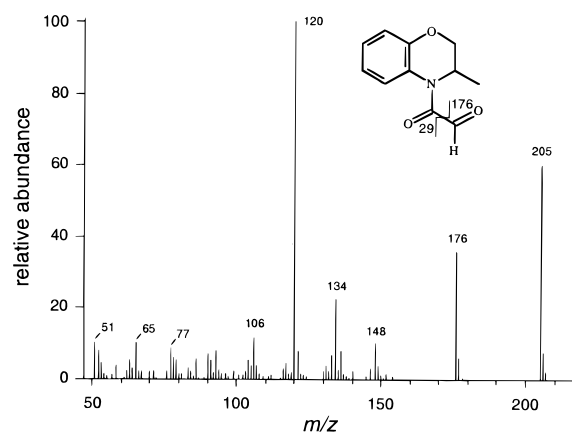


Figure 4. GC-EI/MS spectrum and proposed structure of the formylcarboxamide metabolite. Purification of the formylcarboxamide metabolite prior to GC-EI/MS was accomplished using HPLC according to the gradients and procedures previously described. Gas chromatography of the metabolite was performed prior to entry into the source.

fraction, or both were excluded from the mixture, the reaction did not proceed to an appreciable extent. It was hypothesized that biosynthesis of the *N,N*-diallylgyoxylamide metabolite proceeded through the formation of an unstable glutathione conjugate intermediate, possibly via a pathway analogous to the pathway in Figure 5 (IIa–V). Synthesis of the benoxacor-derived formylcarboxamide compound proceeds nonenzymatically *in vitro* only if conditions (*i.e.* elevated pH) favor the formation of a glutathionyl thiolate anion. Because the cell culture medium used in this study is slightly acidic, and cytosolic or organellar pH values are neutral to slightly acidic, it is doubtful that formation of the formylcarboxamide derivative occurred nonenzymati-

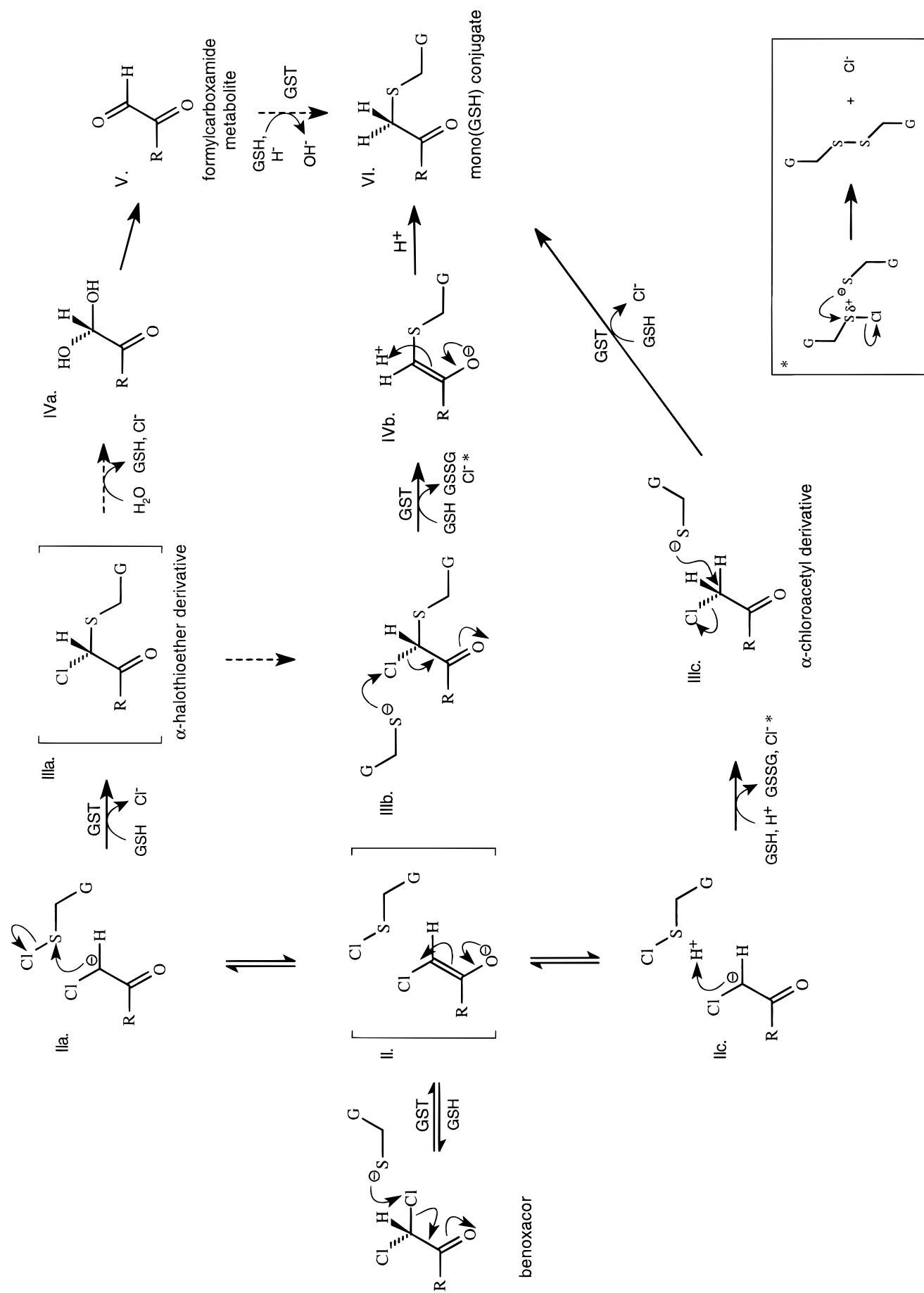


Figure 5. Proposed reaction sequence of the GSH-dependent, GST-catalyzed biosynthesis of the formylcarboxamide metabolite and the GST-catalyzed conjugation of benoxacor to GSH. Details of the reactions are described in the text. R, nitrogen atom of 3,4-dihydro-3-methyl-2H-1,4-benzoxazine; G, glutathione.

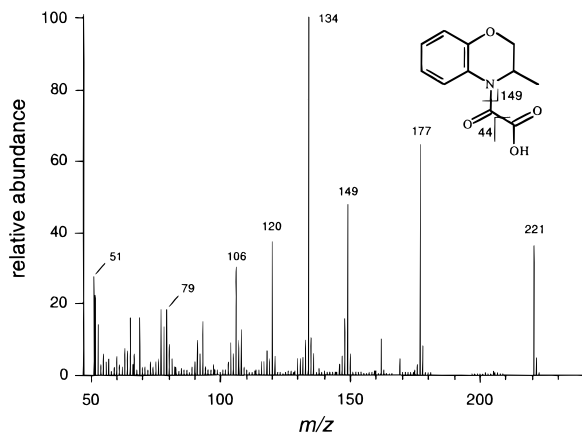


Figure 6. LC-EI/MS spectrum and proposed structure of the carboxy-carboxamide metabolite. The metabolite was purified by HPLC according to the gradients and procedures previously described and then subjected to HPLC using a 40% ACN/0.01% TFA isocratic gradient prior to entering the source as described under Materials and Methods.

cally. Rat liver GST isozyme 3-3 contains a catalytic tyrosine residue at the active site capable of stabilizing the GSH thiolate anion (Ji *et al.*, 1992; Liu *et al.*, 1992). This tyrosine residue is conserved throughout several GST enzymes from different organisms including maize GST I and III (Reinemer *et al.*, 1991). If the catalytic mechanism of plant GSTs is similar to the catalytic mechanism of rat liver GST 3-3, plant GST isozymes could perform the essential function (for the proposed dechlorination mechanism) of stabilizing the glutathionyl thiolate anion and subsequently catalyze the GSH-dependent dechlorination of benoxacor as proposed in Figure 5 (IIa–V).

The reaction sequence in Figure 5 (IIa–V) potentially defines a role for maize GSTs as plant dehalogenase enzymes. In the present context, the dehalogenase activity utilizes GSH as a cofactor instead of a substrate and the activity would appear to be restricted to carbon atoms containing more than one chlorine atom. Whereas dehalogenases (*i.e.* dechlorinase, dehydrochlorinase, reductive dehalogenases) from numerous bacterial species have been well studied (Nagata *et al.*, 1993; Orser *et al.*, 1993; Bader and Leisinger, 1994; Hofer *et al.*, 1994), they have never been reported to occur in plants. It is interesting to note that several of the bacterial dehalogenase deduced amino acid sequences share significant homology with prokaryotic and eukaryotic GSTs (Orser *et al.*, 1993; Bader and Leisinger, 1994).

Carboxy-carboxamide Metabolite [4-(Carboxy-carbonyl)-3,4-dihydro-3-methyl-2H-1,4-benzoxazine]. The spectrum obtained by LC-EI/MS of this metabolite is depicted in Figure 6. The molecular ion was present at m/z 221, while high-mass fragment ions occurred at m/z 177, 149, 134, and 120. The fragment ion at m/z 177 corresponds to the loss of a CO_2 group from the molecular ion. The remaining fragmentation pattern is the same as the previously described benoxacor standard.

The carboxy-carboxamide metabolite may be the result of cytochrome P_{450} monooxygenase-catalyzed hydroxylation of the formylcarboxamide metabolite. Since many aldehyde compounds are autoxidized to carboxylated derivatives, it is also possible that oxygenation occurred during purification of the formylcarboxamide metabolite.

Similar to our results, Miaullis *et al.* (1978) detected a carboxy-carboxamide metabolite, identified as *N,N*-diallyloxamic acid, of the herbicide safener dichlormid

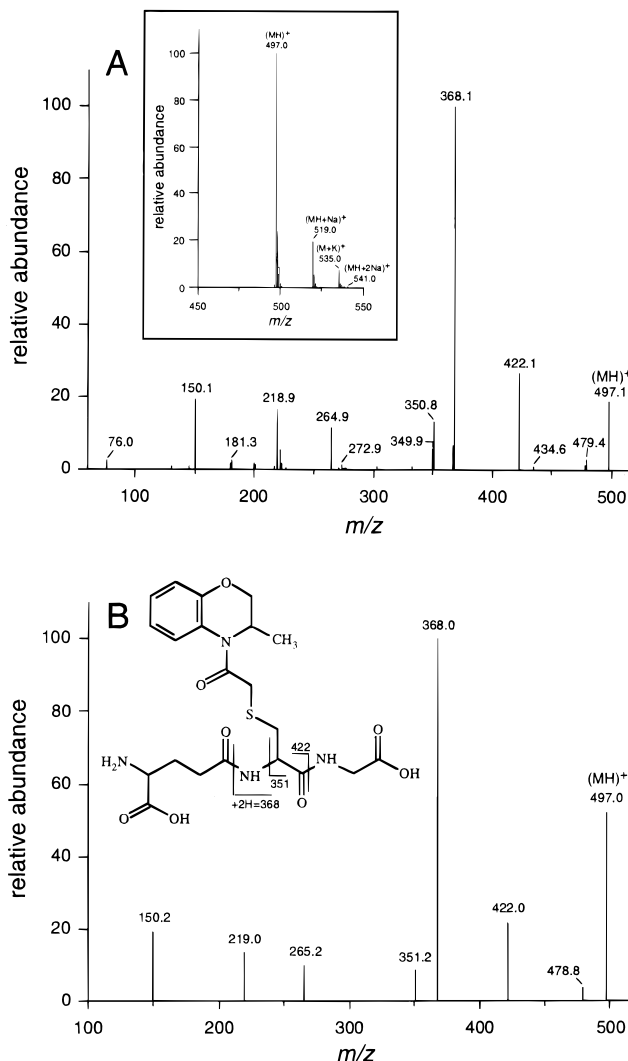


Figure 7. (A) LC-ESI/MS spectrum of the synthetic mono-(GSH) conjugate of benoxacor (inset) and the corresponding MS/MS daughter ion spectrum of the m/z 497 parent ion (main graph). (B) MS/MS daughter ion spectrum of the m/z 497 parent ion obtained by LC-ESI/MS of the extracted mono-(GSH) conjugate metabolite. MS/MS experiments were conducted as described for the synthetic mono-(GSH) conjugate.

in maize seedlings after a 48-h treatment period with [^{14}C]dichlormid. A formylcarboxamide metabolite was not detected, and it was suggested that dichlormid was metabolized to the relatively abundant *N,N*-diallyloxamic acid metabolite through an *N,N*-diallylglycolamide intermediate. The *N,N*-diallylglycolamide intermediate is similar to the hydroxyacetamide benoxacor metabolite present 3 h after benoxacor treatment (Miller *et al.*, 1996) in that it contains an *N*-substituted hydroxyacetamide functional group. Thus, it appears that because similar oxygenated functional groups are present on at least three benoxacor and dichlormid metabolites in maize seedlings and suspension-cultured maize cells, the metabolic fates of these two compounds are at least partially similar.

Mono(GSH) Conjugate [4-(Glutathione-*S*-acetyl)-3,4-dihydro-3-methyl-2H-1,4-benzoxazine]. The LC-ESI/MS spectrum of the synthetic mono(GSH) conjugate of benoxacor is presented in Figure 7A (inset). A protonated molecular ion was present at m/z 497 (MH^+), while sodium adduct ions were detected at m/z 519 ($\text{MH} + \text{Na}^+$) and 541 ($\text{MH} + 2\text{Na}^+$). In addition, a potassium adduct ion was present at m/z 535 ($\text{M} + \text{K}^+$). The MS/MS daughter ion spectrum of the m/z 497 parent ion is

presented in Figure 7A [synthetic mono(GSH) conjugate] and in Figure 7B (extracted metabolite). The fragment ion at m/z 422 ($MH^+ - 74$) is due to the loss of the GSH glycine moiety, while the fragment ion at m/z 368 ($MH^+ - 129$) is due to the loss of the GSH γ -glutamyl moiety from the molecular ion.

1H -NMR COSY spectra (not shown) of the synthetic mono(GSH) conjugate of benoxacor yielded several resonances with chemical shift values from δ 1.5 to 8.0. Specific assignments are as follows: δ 1.51 (C9, d, 3H), 2.47 (glu β C, c, 2H), 2.83 (glu γ C, c, 2H), 3.28 (cys β C, m, 1H), 3.43 (cys β C, m, 1H), 4.04 (C2, m, 1H), 4.12 (C2, m, 1H), 4.14 (glu α C, c, 1H), 4.27 (gly α C, s, 2H), 4.60 (C11, s, 2H), 4.88 (cys α C, t, 1H), 5.06 (C3, b, 1H), 7.34 (C7 and 8, c, 2H), 7.56 (C6, t, 1H), and 7.90 (C5, b, 1H). Because the spectral data obtained at 310 K were broad and ill-defined, the sample was heated to 335 K. The 1H -NMR spectrum of the extracted metabolite was identical to that of the synthetic standard.

Biosynthesis of this metabolite is presumably catalyzed by one or more GST isozymes. It has been previously demonstrated that BMS cells contain GST isozymes capable of utilizing atrazine, metolachlor, and 1-chloro-2,4-dinitrobenzene as substrates (Edwards and Owen, 1986, 1988; Miller *et al.*, 1994). Three postulated pathways describing the biosynthesis of the mono(GSH) conjugate are depicted in Figure 5. Reactions IIa–V have been previously discussed. The formylcarboxamide metabolite could be conjugated to GSH in a GST-catalyzed reaction to form an α -hydroxyl-GSH–benoxacor conjugate. Subsequent reduction of the carbonyl carbon would then yield the mono(GSH) conjugate (Figure 5-VI). Alternatively, the α -chloro carbanion intermediate could abstract a proton (Figure 5-IIc) to form an α -chloroacetyl derivative (Figure 5-IIIc). Subsequent conjugation to GSH, by an S_N2 reaction such as reactions which occur during the metabolism of chloroacetamide herbicides to GSH conjugates (Shimabukuru *et al.*, 1977; Lamoureaux and Rusness, 1990), would yield the mono(GSH) conjugate (Figure 5-VI) of benoxacor. An α -chloroacetamide metabolite was not detected in this study, suggesting that if it is formed, it is a highly reactive intermediate which is rapidly utilized as a substrate by one or more GST isozymes. The final postulated pathway is initiated with the α -halothioether intermediate in Figure 5-IIIb. GST-catalyzed attack of the chlorine by GSH would yield *S*-(chloro)GSH and an *S*-(benoxacor)GSH enolate (Figure 5-IVb). Subsequent proton abstraction would then yield the mono(GSH) conjugate of benoxacor (Figure 5-VI).

Breaux *et al.* (1989) reported that flurazole was metabolized to a GSH conjugate in maize and sorghum seedlings within 2 HAT with [^{14}C]flurazole. This is the only other report of a safener being metabolized to a GSH conjugate *in vivo*. It appears that in addition to inducing increases of GST activity in maize, benoxacor and flurazole, or metabolites thereof, are also substrates for GST isozymes. It is not yet apparent whether benoxacor and flurazole are utilized as substrates by GST enzymes in maize because they contain, or acquire by metabolism, an electrophilic carbon atom susceptible to attack by GSH or whether metabolism to a GSH conjugate, a biosynthetic intermediate, or the GSH conjugate itself is somehow responsible for increases of GST activity.

Figure 8 illustrates the proposed pathway of benoxacor metabolism in suspension cultures of maize 1 HAT

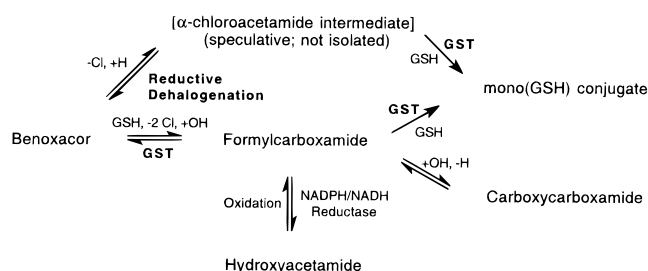


Figure 8. Proposed pathway of [^{14}C]benoxacor metabolism in suspension-cultured maize cells 1 HAT. Benoxacor is either reductively dehalogenated to an α -chloroacetamide derivative and subsequently conjugated to GSH in a GST-catalyzed reaction or converted to the formylcarboxamide metabolite through a GSH-dependent reaction catalyzed by a GST. The formylcarboxamide catabolite is then hydroxylated to the carboxycarboxamide catabolite or conjugated to GSH in a GST-catalyzed reaction. Alternatively, the formylcarboxamide could be reduced to form the hydroxyacetamide metabolite, which was not detected in the present study but was detected 3 HAT.

and is a basic summary of the information presented thus far. Although the di(GSH) conjugate of benoxacor was detected by HPLC of ^{14}C -labeled metabolites extracted from cells treated with [^{14}C]benoxacor for 1 h (Figure 1), it was not detected during mass spectral analyses in this study. Because LC-EI/MS was performed on all metabolite samples in an initial attempt to acquire structural data, it is possible that due to the large mass of the di(GSH) conjugate, it either did not ionize or did not ionize to yield a molecular ion reflecting the size of the intact molecule. The α -hydroxyacetamide metabolite was detected 3 HAT but is included in Figure 8 because it is most likely derived from reduction of the previously discussed formylcarboxamide metabolite. Spectral data and a brief discussion of the α -hydroxyacetamide metabolite are presented elsewhere (Miller *et al.*, 1996).

Because the mono(GSH) conjugate of benoxacor was the most abundant water-soluble metabolite at all time points assayed, and because it is a precursory molecule to the formation of GSH-related metabolites identified by Miller *et al.* (1996), it appears that the major pathway by which benoxacor is metabolized in maize cell suspension cultures is through conjugation with GSH.

ABBREVIATIONS USED

ACN-d₃, deuterated acetonitrile; BMS, Black Mexican Sweet; COSY, correlative spectroscopy; cpm, counts per minute; D₂O, deuterated water; GC-EI/MS, gas chromatography–electron impact mass spectrometry; GSH, glutathione; GST-C, glutathione *S*-transferase capable of utilizing 1-chloro-2,4-dinitrobenzene as a substrate; h, hour or hours; HAT, hours after treatment; HPLC, high-performance liquid chromatography; LC-EI/MS, liquid chromatography–electron impact mass spectrometry; LC-ESI/MS, liquid chromatography–electrospray ionization mass spectrometry; LSC, liquid scintillation counting; MeOH, methanol; NMR, nuclear magnetic resonance; SPE, solid-phase extraction; TAPS, *N*-tris-[hydroxymethyl]methyl-3-aminopropanesulfonic acid; TFA, trifluoroacetic acid; TLC, thin layer chromatography.

ACKNOWLEDGMENT

We thank William Siems in the Washington State University Department of Chemistry for conducting a portion of the GC and LC-EI/MS analysis.

LITERATURE CITED

- Bader, R.; Leisinger, T. Isolation and characterization of the *Methylophilus* sp. strain DM11 gene encoding dichloromethane dehalogenase/glutathione S-transferase. *J. Bacteriol.* **1994**, *176* (12), 3466–3473.
- Breaux, E. J.; Hoobler, M. A.; Patanella, J. E.; Leyes, G. A. Mechanism of action of thiazole safeners. In *Crop Safeners for Herbicides—Development, Uses, and Mechanisms of Action*; Hatzios, K. K., Hoagland, R. F., Eds.; Academic Press: New York, 1989.
- Butt, V. S.; Lamb, C. J. Oxygenases and the metabolism of plant products. In *The Biochemistry of Plants—A Comprehensive Treatise, Vol. 7, Secondary Plant Products*, Conn, E. E., Ed.; Academic Press: New York, 1981.
- Clark, A. G.; Shamaan, N. A. Evidence that DDT-dehydrochlorinase from the house fly is a glutathione S-transferase. *Pestic. Biochem. Physiol.* **1984**, *22*, 249–261.
- Dean, J. V.; Gronwald, J. W.; Anderson, M. P. Glutathione S-transferase activity in nontreated and CGA-154281-treated maize shoots. *Z. Naturforsch.* **1991**, *46c*, 850–855.
- Donaldson, R. P.; Luster, D. G. Multiple forms of plant cytochrome P-450. *Plant Physiol.* **1991**, *96*, 669–674.
- Dutka, F. Bioactive chemical bond systems in safeners and prosafeners. *Z. Naturforsch.* **1991**, *46C*, 805–809.
- Edwards, R.; Owen, W. J. Comparison of glutathione S-transferases of *Zea mays* responsible for herbicide detoxification in plants and suspension-cultured cells. *Planta* **1986**, *169*, 208–215.
- Edwards, R.; Owen, W. J. Regulation of glutathione S-transferases of *Zea mays* in plants and cell cultures. *Planta* **1988**, *175*, 99–106.
- Fuerst, E. P.; Irzyk, G. P.; Miller, K. D. Partial characterization of glutathione S-transferase isozymes induced by the herbicide safener benoxacor in maize. *Plant Physiol.* **1993**, *102*, 795–802.
- Hofer, B.; Backhaus, S.; Timmis, K. N. The biphenyl/polychlorinated biphenyl-degradation locus (*bph*) of *Pseudomonas* sp. LB400 encodes four additional metabolic enzymes. *Gene* **1994**, *144*, 9–16.
- Irzyk, G. P.; Fuerst, E. P. Purification and characterization of a glutathione S-transferase from benoxacor-treated maize (*Zea mays*). *Plant Physiol.* **1993**, *102*, 803–810.
- Ji, X.; Zhang, P.; Armstrong, R. N.; Gilliland, G. L. The three-dimensional structure of a glutathione S-transferase from the mu gene class. Structural analysis of the binary complex of isoenzyme 3-3 and glutathione at 2.2 Å resolution. *Biochemistry* **1992**, *31*, 10169–10184.
- Jones, O. T. G.; Caseley, J. C. Role of cytochrome P450 in herbicide metabolism. *Proc. Brighton Crop Prot. Conf., Weeds* **1989**, *9B-1*, 1175–1184.
- Kömives, T.; Hatzios, K. K. Chemistry and structure-activity relationships of herbicide safeners. *Z. Naturforsch.* **1991**, *46c*, 798–804.
- Lamoureux, G. L.; Rusness, D. G. Selected aspects of glutathione conjugation research in herbicide metabolism and selectivity. In *Sulfur Nutrition and Sulfur Assimilation in Higher Plants*; Rennenberg, H., Brunhold, C. H., DeKok, L. J., Stulen, I., Eds.; SPB Academic Press: The Hague, 1990.
- Liu, S.; Zhang, P.; Ji, X.; Johnson, W. W.; Gilliland, G. L.; Armstrong, R. N. Contribution of tyrosine-6 to the catalytic mechanism of isoenzyme 3-3 of glutathione S-transferase. *J. Biol. Chem.* **1992**, *267* (7), 4296–4299.
- Martin, J. L.; Gross, B. J.; Morris, P.; Pohl, L. R. Mechanism of glutathione-dependent dechlorination of chloramphenicol and thiamphenicol by cytosol of rat liver. *Drug Metab. Dispos.* **1980**, *8*, 371–375.
- Miaullis, J. B.; Thomas, V. M.; Gray, R. A.; Murphy, J. J.; Hollingworth, R. M. Metabolism of R-25788 (*N,N*-diallyl-2,2-dichloroacetamide) in corn plants, rats, and soil. In *Chemistry and Action of Herbicide Antidotes*; Pallos, F. M., Casida, J. E., Eds.; Academic Press: London, England, 1978.
- Miller, K. D.; Irzyk, G. P.; Fuerst, E. P. Benoxacor treatment increases glutathione S-transferase activity in suspension cultures of *Zea mays*. *Pestic. Biochem. Physiol.* **1994**, *48*, 123–134.
- Miller, K. D.; Irzyk, G. P.; Fuerst, E. P.; McFarland, J. E.; Barringer, M.; Cruz, S.; Eberle, W. J.; Föry, W. Identification of metabolites of the herbicide safener benoxacor isolated from suspension-cultured *Zea mays* cells 3 and 24 h after treatment. *J. Agric. Food Chem.* **1996**, *44*, XXXX–XXXX.
- Nagata, Y.; Nariya, T.; Ohtomo, R.; Fukuda, M.; Yano, K.; Takagi, M. Cloning and sequencing of a dehalogenase gene encoding an enzyme with hydrolase activity involved in the degradation of γ -hexachlorocyclohexane in *Pseudomonas paucimobilis*. *J. Bacteriol.* **1993**, *175* (20), 6403–6410.
- Orser, C. S.; Dutton, J.; Lange, C.; Jablonski, P.; Xun, Luying; Hargis, M. Characterization of a *Flavobacterium* glutathione S-transferase gene involved in reductive dechlorination. *J. Bacteriol.* **1993**, *175* (9), 2640–2644.
- Prapanthadara, L.; Hemingway, J.; Ketterman, A. J. Partial purification and characterization of a glutathione S-transferase involved in DDT resistance from the mosquito *Anopheles gambiae*. *Pestic. Biochem. Physiol.* **1993**, *47*, 119–133.
- Reinemer, P.; Dirr, H. W.; Ladenstein, R.; Schaffer, J.; Gally, O.; Huber, R. The three-dimensional structure of class π glutathione S-transferase in complex with glutathione sulfonate at 2.3 Å resolution. *EMBO J.* **1991**, *10* (8), 1997–2005.
- Shimabukuro, R. H.; Lamoureux, G. L.; Frear, D. S. Glutathione conjugation: a mechanism for herbicide detoxification and selectivity in plants. In *Chemical Action of Herbicide Antidotes*; Pallos, F. M., Casida, J. E., Eds.; Academic Press: New York, 1977.
- Viger, P. R.; Eberlein, C. V.; Fuerst, E. P.; Gronwald, J. W. Effects of CGA-154281 and temperature on metolachlor absorption and metabolism, glutathione content, and glutathione S-transferase activity in corn (*Zea mays*). *Weed Sci.* **1991**, *39*, 324–328.

Received for review August 10, 1995. Revised manuscript received April 19, 1996. Accepted May 9, 1996.[®]

JF950542D

[®] Abstract published in *Advance ACS Abstracts*, August 1, 1996.